

Structural Sensitivity of 1,2-Aryl Rearrangements in Triarylvinyl Cations: Bridged Transition States vs Bridged Intermediates and Inversion vs Helicity Retention

Hiroshi Yamataka,^{*,†} Silvio E. Biali,^{*,‡} and Zvi Rappoport^{*,‡,§}

Institute of Scientific and Industrial Research, Osaka University, Ibaraki, Osaka 567, Japan, and Department of Organic Chemistry and Minerva Center for Computational Quantum Chemistry, The Hebrew University of Jerusalem, Jerusalem 91904, Israel

Received March 25, 1998

Triarylvinyl cations (**1**) are reactive intermediates that can undergo 1,2-aryl migrations across the double bond via bridged species (**2**).¹ Stereochemical and kinetic evidence indicate that in the solvolysis of Ar¹Ar²C=C(X)-Ar systems there is no neighboring β -Ar participation and that the products are derived from attack of the solvent (or nucleophile) on the linear ion **1**. Although a bridged species **2** must appear on the reaction coordinate of the rearrangement, it is unknown whether it is a transition state or a discrete intermediate and what the linear/bridged ion energy gap is.^{2,3}

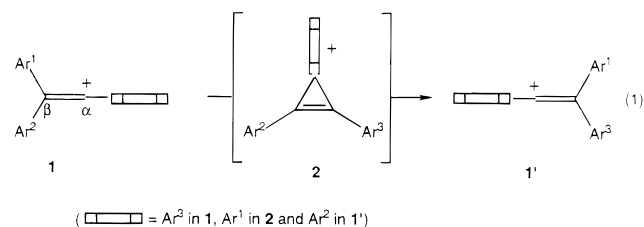
An additional unknown feature of the 1,2-aryl migration in triarylvinyl cations concerns a hitherto unexplored aspect of its stereochemistry. In the linear ion **1**, the α -ring (Ar³) is perpendicular to the double bond plane and conjugation with the cationic p orbital is maximal, while in **2** the migrating ring (Ar¹) is perpendicular to the double bond plane in order to simultaneously overlap the partially positively charged migration origin and terminus. If all rings possess local C₂ symmetry, the ions are achiral when the nonmigrating rings adopt coplanar or perpendicular arrangements with the double bond. Starting from an achiral linear ion **1**, either an achiral or chiral helical species **2**^{4–6} can be a priori formed. In contrast, a chiral "propeller" conformation of **1** results if the Ar–C=C torsional angles are 0° < $|\varphi|$ < 90° and both β -rings are twisted in the same sense.⁶ The two enantiomeric propeller forms differ in the sense of twist of the rings (i.e., the "helicity"). A chiral ion **1** may enantiomerize by rotation of the β -rings around the =C–Ar bonds. There are several such processes, which a priori

Table 1. Calculated Relative Energies^a of the Bridged Species **4a–d**

method	4a	4b	4c	4d
HF/3-21G	17.2 (17.2) ^b	7.4 (9.1) ^b	26.5 ^b	11.3 ^b
B3LYP/3-21G//HF/3-21G ^c	11.9 (11.9)	4.5 (5.6)	20.6	5.8
B3LYP/3-21G	11.5 (11.5) ^b	4.7 (5.7) ^b	19.8 ^b	5.4 ^b
B3LYP/6-31G*/B3LYP/3-21G ^d	7.0 (7.2)	0.1 (2.0)	15.3	2.1
B3LYP/6-31G*	6.8			

^a Energies (in kcal mol⁻¹) are relative to the corresponding open ion. ^b Transition state of the rearrangement. ^c Single-point calculations using the HF/3-21G geometries. ^d Single-point calculations using the B3LYP/3-21G geometries.

are expected to possess a low barrier and one of which may well be the threshold process for enantiomerization.⁶ Here, we are interested in another, probably a higher energy process, which can independently modify the helicity. This process is the 1,2-aryl migration in which along the reaction coordinate **1** → **2** → **1'** (eq 1)⁷ the torsional angles of all three rings change. The most convenient approach to study this process is computational. The goals of the present study were (a) to determine whether the bridged carbocationic species **2** is an intermediate or a transition state, (b) to assess the linear/bridged ion energy gap, and (c) to determine the possible fates of helical and nonhelical precursors during the degenerate 1,2-aryl rearrangements.⁸



The stereochemistry of the degenerate 1,2-aryl migrations in **1** was probed by ab initio molecular orbital (MO) as well as density functional theory (DFT) calculations (Table 1).^{9,10} We had chosen for Ar¹, Ar², and Ar³ various combinations of the least bulky (Ph) and highly bulky (mesityl and 2,6-xylyl) aryl groups, since we expected that they would lead to different preferred conformations in the ions **3a–d** and the corresponding bridged species **4a–d**.^{10b} The choice of the computation method was largely dictated by the large number of atoms of our systems. Compounds **3a–d** and **4a–d** were first optimized at the

(7) The rectangular structure indicates an aryl ring perpendicular to the double bond plane.

(8) For a stereochemical analysis of 1,2-aryl rearrangements in triarylvinyl cations with Ar¹ ≠ Ar² ≠ Ar³, see: Biali, S. E.; Rappoport, Z. *J. Am. Chem. Soc.* **1984**, *106*, 477.

(9) Ab initio MO calculations were carried out by using the GAUSSIAN 94 program (Frisch, M. J.; Trucks, G. W.; Schlegel, H. B.; Gill, P. M. W.; Johnson, B. G.; Robb, M. A.; Cheeseman, J. R.; Keith, T. A.; Peterson, G. A.; Montgomery, J. A.; Raghavachari, K.; Al-Laham, M. A.; Zakrzewski, V. G.; Ortiz, J. V.; Foresman, J. B.; Cioslowski, J.; Stefanov, B. B.; Nanayakkara, A.; Challacombe, M.; Peng, C. Y.; Ayala, P. Y.; Chen, W.; Wong, M. W.; Andress, J. L.; Replogle, E. S.; Gomperts, R.; Martin, R. L.; Fox, D. J.; Binkley, S.; Defrees, D. J.; Baker, J.; Stewart, J. P.; Head-Gordon, M.; Gonzalez, C.; Pople, J. A. *GAUSSIAN 94*, revision C.2; Gaussian Inc.: Pittsburgh, PA, 1995). All structures were fully optimized at the HF/3-21G level without any symmetry constraint. Transition states were confirmed by vibrational frequency calculations to have only one imaginary frequency.

(10) For previous ab initio calculations of triarylvinyl cations, see: (a) Kobayashi, S.; Hori, Y.; Hasako, T.; Koga, K.; Yamataka, H. *J. Org. Chem.* **1996**, *61*, 5274. (b) Yamataka, H.; Aleksiuk, O.; Biali, S. E.; Rappoport, Z. *J. Am. Chem. Soc.* **1996**, *118*, 12580.

[†] Osaka University.

[‡] Department of Organic Chemistry, Hebrew University.

[§] Minerva Center for Computational Quantum Chemistry, Hebrew University.

(1) (a) Stang, P. J.; Rappoport, Z.; Hanack, M.; Subramanian, L. R. *Vinyl Cations*; Academic Press: New York, 1979. (b) *Dicoordinated Carbocations*; Rappoport, Z., Stang, P. J., Eds.; Wiley: Chichester, 1997.

(2) For a review on rearrangements of vinyl cations see ref 1a, chapter 6.

(3) Recent calculations on the parent H₂CCH cation indicate that the bridged ion is of lower energy than the open ion. For a review see Apeloig, Y.; Müller, T. in ref 1b, chapter 2.

(4) In an achiral medium, either of the two helicities can be formed.

(5) For a review on molecular propellers and helical structures see: Mislow, K. *Acc. Chem. Res.* **1976**, *9*, 26. Meurer, K. P.; Vögtle, F. *Top. Curr. Chem.* **1985**, *127*, 1–76.

(6) For a recent review on vinyl propellers see: Rappoport, Z.; Biali, S. E. *Acc. Chem. Res.* **1997**, *30*, 307.

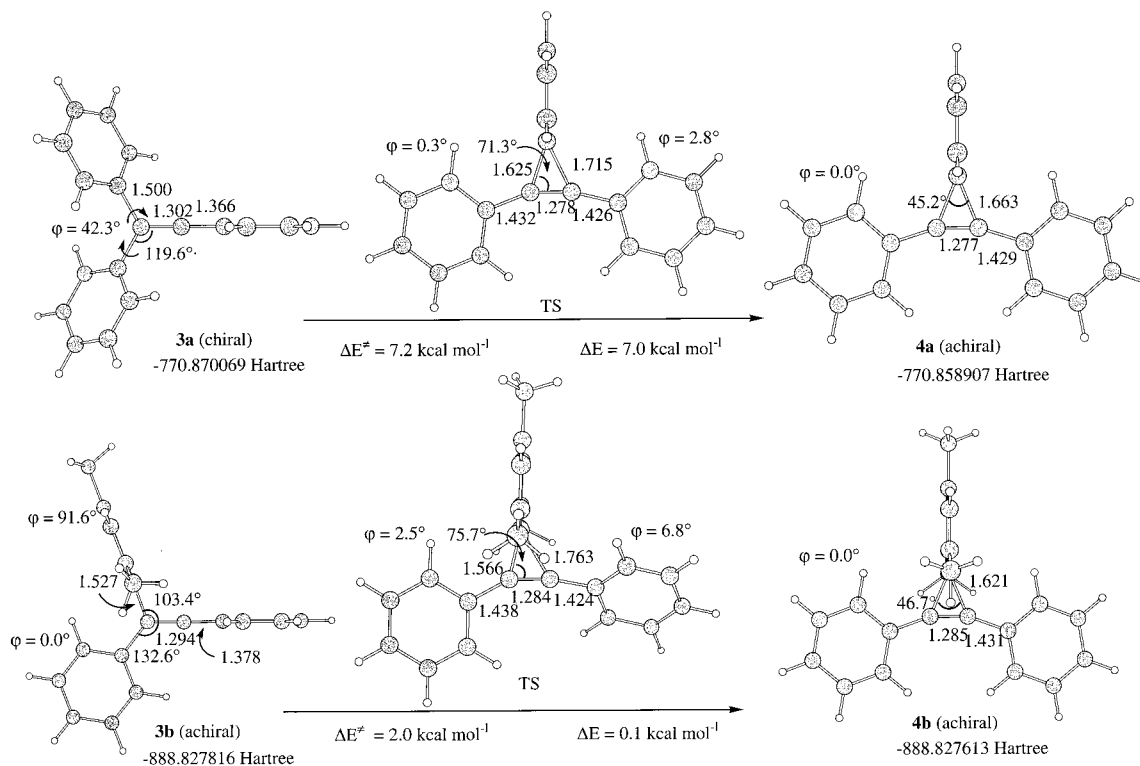
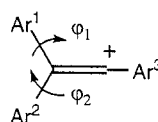
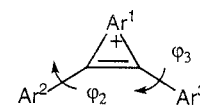


Figure 1. Calculated geometries, energies (in hartrees), energy differences between the bridged and open ions (ΔE , in kcal mol⁻¹), and activation barriers (ΔE^\ddagger , in kcal mol⁻¹) for the **3a** → **4a** and **3b** → **4b** processes. The bridged ion **4a** and the transition state leading to it are nearly isoenergetic. Bond lengths are in angstroms; angles are in degrees. φ denotes the torsional angles $C_\alpha-C_\beta-C_{\text{ipso}}-C_{\text{ortho}}$ in **3** and **4**.

HF/3-21G level of theory. Local minima and transition-state structures were identified by means of a full analysis of the vibrational modes at those stationary points. To incorporate the effect of electron correlation, geometry optimization and energy calculations were also carried out with nonlocal hybrid DFT¹¹ at the B3LYP level.¹² The structures obtained at this level of theory are basically similar to those obtained at HF/3-21G, which are given below in square brackets, although some of the dihedral angles differ considerably. As can be seen in Table 1, for all ions, the DFT calculations give smaller linear/bridged ion energy gaps than the HF/3-21G MO calculations. It should also be noted that the optimized B3LYP/3-21G energy gap is quite similar to that obtained from single-point energy calculations at B3LYP/3-21G on the HF/3-21G optimized geometries. To incorporate the effect of polarization functions, single-point energy calculations were carried out with a larger basis set (6-31G*) using the B3LYP/3-21G optimized geometries. The results are summarized in Table 1,¹³ which also lists the B3LYP/6-31G* optimized relative energy of **4a** compared to that of **3a**. The calculated B3LYP/6-31G* energy gap (cf. Table 1) compares favorably with the B3LYP/6-31G**/B3LYP/3-21G result. For the discussion below, we will use throughout the energies obtained at B3LYP/6-31G**/B3LYP/3-21G.



- 3a** Ar¹ = Ar² = Ar³ = Ph
3b Ar¹ = Mes, Ar² = Ar³ = Ph
3c Ar² = Ar³ = Mes, Ar¹ = Ph
3d Ar¹ = Ar² = Ar³ = Xyl
3e Ar¹ = An, Ar² = Ar³ = Ph
3f Ar¹ = Ar² = Ar³ = An
3g Ar² = Ar³ = An, Ar¹ = Ph



- 4a** Ar¹ = Ar² = Ar³ = Ph
4b Ar¹ = Mes, Ar² = Ar³ = Ph
4c Ar¹ = Ph, Ar² = Ar³ = Mes
4d Ar¹ = Ar² = Ar³ = Xyl

Mes = 2,4,6-Me₃C₆H₂, Xyl = 2,6-MeC₆H₃, An = 4-MeOC₆H₄

Calculations for the least crowded triphenylvinyl cation **3a** indicate that its α -ring is perpendicular to the double bond plane, with Ar¹ and Ar² adopting a chiral propeller conformation ($\varphi_1 = \varphi_2 = 42.3^\circ$ [45.8°]). The achiral bridged species **4a**, in which the Ar² and Ar³ rings are coplanar with the double bond, lies 7.0 kcal mol⁻¹ above **3a** and only 0.2 kcal mol⁻¹ below the transition state leading to it (Figures 1 and 2).¹⁴ As a result of the shallowness of the potential energy surface near **4a**, we cannot unequivocally determine whether it indeed corresponds to a local minimum. If **4a** is a transition state, the outcome of the rearrangement should be inversion of the helicity, while if **4a** represents a chiral discrete intermediate, either helicity is possible in **1'**.¹⁵ According to these calculations, **4b** corresponds to a discrete intermediate that lies 0.1 kcal mol⁻¹ above **3b** and 2.0 kcal mol⁻¹ below the transition state leading to it. Both **4b** ($\varphi_2 = \varphi_3 = 0^\circ$ [0°]) and **3b** ($\varphi_1 = 91.6^\circ$ [91.4°], $\varphi_2 = 0^\circ$ [0.0°])¹⁶ adopt nonpropeller achiral conformations; i.e.,

(11) Becke, A. D. *J. Chem. Phys.* **1993**, *98*, 5648.

(12) (a) Becke, A. D. *Phys. Rev.* **1988**, *A38*, 3098. (b) Lee, C.; Yang, W.; Parr, R. G. *Phys. Rev.* **1988**, *B37*, 785.

(13) Polarization functions and correlation effects are known to relatively stabilize the bridged ions compared with the linear ions. See: Hehre, W. H.; Radom, L.; Schleyer, P. v. R.; Pople, J. A. *Ab Initio Molecular Orbital Theory*; Wiley: New York, 1986; p 379. Compare also ref 3. Schreiner, P. R.; Schleyer, P. v. R.; Schaefer, H. F. *J. Org. Chem.* **1997**, *62*, 4216.

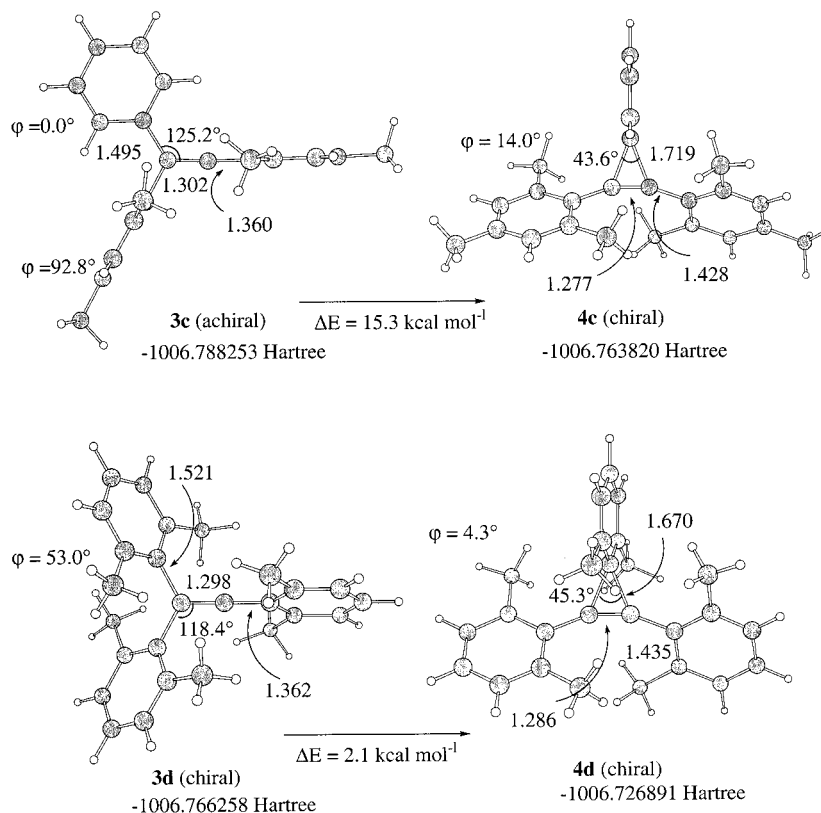


Figure 2. Calculated geometries, energies (in hartrees), and barriers (ΔE^\ddagger , in kcal mol⁻¹) for the **3c** → **4c** and **3d** → **4d** processes. The bridged species represent transition states.

helicity is absent in both the linear ion and the intermediate ion formed in the rearrangement.

The situation changes when the nonmigrating aryl rings become bulkier. According to the calculations, the open ion **3d** is chiral ($\varphi_1 = \varphi_2 = 53.0^\circ$ [52.5°]), while **3c** is achiral ($\varphi_1 = 90^\circ$ [92.2°], $\varphi_2 = 0^\circ$ [0°]). The bridged ions **4c** and **4d** no longer lay in a shallow minimum but instead represent saddle points located 15.3 and 2.1 kcal mol⁻¹ above **3c** and **3d**, respectively. Both transition states are chiral ($\varphi_2 = \varphi_3 = 14.0^\circ$ [31.0°] and 4.3° [13.7°] for **4c** and **4d**, Figure 3), since in both ions steric interactions involving *o*-Me groups preclude a coplanar arrangement of the Ar² and Ar³ rings with the double bond. Progress along the reaction coordinate of the degenerate rearrangement of the achiral **3c** first generates helicity in the **1** → **2** stage (since **2** is chiral), which is later destroyed in the **2** → **1'** stage.

The bridged ion **4d** possesses a chiral propeller conformation, a fact that is compatible with either helicity

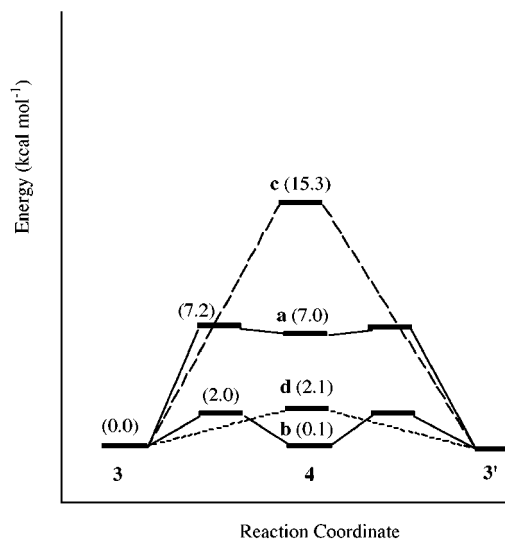


Figure 3. Reaction profiles for 1,2-aryl migrations. Numbers are relative energies in kcal mol⁻¹ for the species **a** (Ph₂C=CPh), **b** (Mes(Ph)C=CPh), **c** (Mes(Ph)C=CMes), and **d** (Xyl₂C=CXyl). For simplicity, the energies of all the linear ions are given as identical.

retention or inversion during the rearrangement. However, since in **4d** the passage of the two rings Ar² and Ar³ through the double bond plane is sterically hindered by the *o*-methyl groups, it is most likely that the helicity is retained during the rearrangement.

The order of the barriers for the rearrangement (in kcal mol⁻¹) of **3b** (2.0) ≤ **3d** (2.1) < **3a** (7.2) < **3c** (15.3) qualitatively parallels the order of the experimental extents of degenerate rearrangements (i.e., the ratio of rearranged to unrearranged product) in analogues where

(14) This situation is reminiscent of the conformational behavior of 1,2-diarylcyclopropanes, which in the absence of ortho substituents adopt a planar conformation. (a) Gur, E.; Biali, S. E.; Rappoport, Z.; Kaftory, M. 56th Annual Meeting of the Israel Chemical Society, Jerusalem, February 11–12, 1991; Abstract 98. (b) Gur, E.; M.Sc. Thesis, The Hebrew University of Jerusalem, 1991.

(15) Retention and inversion of the helicity mean that **1** and **1'** possess an identical or opposite (clockwise or counterclockwise) sense of twist of the rings, respectively. When the achiral **2** is a transition state, the initial direction of rotation of the rings (clockwise or counterclockwise) should not change after crossing the saddle point, and therefore there should be inversion of the helicity. On the other hand, if **2** is an achiral intermediate of a finite lifetime, either helicity might be generated in the **2** → **1'** step, since **2** does not have a "memory" of the direction of rotation in the step **2** → **1**.

(16) The mesityl ring in **3b** is nonplanar and slightly folded (its C_α–C_β–C_{ipso}–C_{ortho} torsional angles are –91° and +91°), which allows for an achiral conformation, even if the φ_1 values are not exactly 90°.

the electron-donating *p*-anisyl replaces the electron-donating 2,6-xylyl group [**3e** (93%) > **3f** (35%) > **3a** (13.4%) > **3g** (<3%) in AcOH].¹⁷ Both series reflect the increased stability of the bridged compared with the linear species as the stabilization of the transition state increases by the bridging group at the expense of the stabilization of the linear ion.¹⁸

According to the calculations, whether the bridged ionic species is a transition state or an intermediate in a shallow minimum depends on the stability of **2** relative

(17) Reference 1a, pp 419–420.

(18) Solution data¹ indicate that bridged species are not observed in the solvolysis of triarylvinyl systems.^{2b} However, when the migrating group is the strongly electron-donating and negatively charged *p*-phenoxide group, the neutral analogue of the bridged species is isolable ((a) Ohba, H.; Ikeda, T.; Kobayashi, S.; Taniguchi, H. *J. Chem. Soc., Chem. Commun.* **1980**, 988. (b) Ikeda, T.; Kobayashi, S.; Taniguchi, H. *Synthesis* **1982**, 393. (c) Ikeda, T.; Kobayashi, S.; Taniguchi, H. *Chem. Lett.* **1982**, 387, 391). The X-ray structure of such an analogue has been recently determined (Kobayashi, S.; Boese, R.; Stanger, A.; Rappoport, Z. Unpublished results).

to **1**. When **1** is strongly stabilized at C_α (as in **3c** and **3d**) and **2** is sterically crowded, the bridged species is calculated to be a transition state rather than a minimum on the potential energy surface.

Conclusions. Dependent on the substituents, the bridged species **4** may be an intermediate or a transition state on the potential energy surface for the rearrangement. Dependent on the bulk of the aryl ring substituents, the precursor ion **1** and the bridged species **2** may be chiral or achiral. All four combinations of chiral/achiral **1** and **2** were found computationally. In the lowest energy rearrangement across the double bond of triarylvinyl cations, helicity inversion and retention are possible.

Acknowledgment. This research was supported by the Israel–USA Binational Science Foundation (BSF).

JO980556T